Heritage Science

RESEARCH

Open Access

Macrokinetics of the deterioration of cement-based grouting material for predicting its service life under acid rain attack

Wenjing Hu[1], Shiqiang Fang[1,2*], Lina Xie[1], Xueqiang Chen[1] and Bingjian Zhang[2]

Abstract

Cement-based grouting material is widely used to reinforce the unsafe rock and control seepage of rock-carved relics although it is considered inappropriate in protection of ancient sites. As this approach is irreversible, a longer service life is desirable for the grouting material and methods to predict the service life are needed. Here we propose a universal formula based on the dissolved amount of calcium ion to predict the deterioration rate of cement-based grout caused by acid deposition in the laboratory. The experimental results showed that the dissolved amount of calcium ion had a linear relationship with *ln*T and the pH value, with better accuracy when the pH value was greater than 3.0. This work maybe could provide a facile and quantitative method to help us predict the service life of cement-based grouting material under acid rain attack outdoors.

Keywords Cement, Macrokinetics, Reaction rate constant, Acid rain, Ca^{2+} ion

Introduction

Rock carving, an ancient method of documenting historical events, expressing emotions and beliefs, has been transmitted across diverse regions worldwide throughout the course of human civilization. Presently, these invaluable cultural relics continue to be prominently visible in various regions around the globe [1–7]. In general, these rock-carved cultural relics were frequently excavated in steep slopes composed of what was known as "weak rocks" [8]. The relatively low strength value of such steep slopes facilitated the excavation and carving process; however, it compromised the overall stability of these slopes (such as cracking, water seepage, collapse, and falling rocks), thereby posing a threat to both the preservation of stone relics and the safety of tourists. In order to enhance the protection and exhibition of these rock-carved relics for public viewing, cultural heritage conservators had undertaken extensive efforts over recent decades, including implementing a monitoring system [2, 4, 6, 9–11], reinforcing unstable rocks [1, 12, 13], managing water infiltration [7, 14, 15], transforming the surrounding landscape [4, 10, 16], and so on.

Among the various factors influencing the preservation of rock-carved relics and cliff stability, water seepage emerged as a pivotal element [8]. This was due to the fact that water infiltration could result in the dissolution of cementitious materials within rocks possessing higher solubility, while part of substances prone to water absorption expand upon contact with water, thereby leading to rock structure deterioration and strength reduction [17–20]. Consequently, control of water seepage played

*Correspondence:
Shiqiang Fang
704747260@qq.com; fangsq@zju.edu.cn
[1] Centre for the Protection of Cultural Property and New Economic Research Institute, Ningbo University of Finance & Economics, Ningbo 315175, People's Republic of China
[2] Department of Cultural Heritage and Museology, Zhejiang University, Hangzhou 310028, People's Republic of China

a pivotal role in safeguarding rock-carved cultural relics. The approaches encompassed the construction of water drainage system as measures to mitigate surface runoff and ground water infiltration [8, 21], utilization of chemical grout for sealing exposed fractures [13, 22], and occasionally employing a combination of both strategies [3, 23]. It is well known that the grouting is a non-reversible technique, yet it has been proven to be highly effective and is predominantly embraced by conservators for the intervention of rock-carved cultural relics. Depending on the actual state of rock-carved cultural relics, the specific objectives of intervention, and the allocated financial resources, cement-based grouts with enhanced strength and superior water resistance were commonly utilized in this particular field instead of lime-based grouts typically employed for safeguarding mosaics, frescoes, and decorative elements [13]. Similar to the grouting process employed in other stone masonries, prior to commencing the actual grouting operation, comprehensive tests would be conducted on various properties of the grouting material, including fluidity, stability, and compressive strength. These tests would guide us in selecting an appropriate grouting material or ratio. However, there was a paucity of studies assessing the service life of grout materials, which hindered our comprehensive understanding of the efficacy of this intervention and the potential risks for future conservation efforts.

As is well known, the acid resistance of cement-based material is low, because the hydration products of cement usually contain alkaline substances. Once the alkaline substances occur neutralization reaction with H^+ ion in the acidic substances, the matters which are stabilized by alkaline situation (like hydrated calcium silicate, calcium aluminate, calcium sulfoaluminate) will dissolve and lead to the further deterioration of cement-based material. In the past decades, acid rain problem was increasingly severe with the rapid industrialization and urbanization around the world. For instance, the southern region of China had become the third region in the world seriously affected by acid rain during the past decades following Northeast America and Central Europe [24]. And the acid precipitation had occurred in about 40% of the entire territory [25]. Unfortunately, these heavily acid rain polluted areas were home to a significant amount of rock-carved relics. In contrast to the independent stone masonries, the intricate internal joint structure of the steep slopes necessitated prolonged contact between grout material and infiltrating precipitation. Consequently, despite implementing surface treatment post-grouting to prevent direct exposure of the grout material, acid rain still compromised its stability. Therefore, it was imperative to investigate and establish an effective methodology for evaluating and predicting the service life of cement-based grout materials in acidic environments, which held significant practical implications. However, in fact, it was difficult to predict the failure rate of cement-based materials because the failure process was a complex process. It included both physical damage caused by volume change of soluble salt and water molecules crystals, and chemical damage caused by internal ion loss [26]. In addition, the quality of raw materials, preparation technology, stress conditions and types of erosive ions also would affect the failure process of materials [27].

At present, the methods commonly used to evaluate the failure degree of cement-based materials subjected to acid rain erosion are as follows: *(1) Compressive strength* [28]. The change of compressive strength of cement specimens before and after acid rain erosion was simulated to evaluate the quality of cement-based materials. However, some studies believed that when the cement was eroded by acid rain at the beginning, the neutral substance formed had a protective effect on the cement, and the strength of the cement might not decrease [29]. Therefore, although this method was simple and easy to operate, its accuracy might not be good. *(2) Mass loss* [30, 31]. The acid rain erosion of cement-based material was evaluated by measuring the weight change of cement specimens. Under the normal circumstance, the mass loss rate was very slow when the pH > 3, thus, we had to increase the acidity of acid rain in the simulation [32]. *(3) Ion leaching* [28, 33]. Acid rain and cement reactions release calcium, silicon plasma and compounds from the cement. The degradation of the cement could be quantitatively studied by measuring these dissolved substances. *(4) Neutralization degree* [29, 34]. Acid rain and cement have neutralization reaction. The acid and alkali of cement can be tested to estimate the acid rain erosion degree. It should be noted that this method assumes that the neutralization reaction develops from the outside to the inside in the cement specimens because that's not always the case with carbonization [35]. *(5) Structural changes* [36, 37]. Acid rain reacts with cement to produce micropores in solidified cement specimens. These structural changes can be observed by CT scanning and other methods. This method has high requirements on the instrument.

In general, each approach has its own advantages and disadvantages. Considering that the measurement of ion dissolution can monitor the cement degradation process in real-time and quantitatively, thus, in this work, we reported a novel method of using the dissolving-out amount of Ca^{2+} from cement-based grouting materials under the mimical acid rain to quantitatively or semi-quantitatively predict their service life. The experimental data obtained from this work could also be used for analog computation cement failure model by computer.

Experimental scheme

Materials

Ordinary Portland cement was purchased from Yuhang QianChao Cement Co. (Hangzhou, China) and its strength grade was 42.5. The elementary composition of this ordinary Portland cement was summarized in Table 1 using an energy spectrum instrument (EDS, Metek, Octane Elect Plus). Water reducer was purchased from the building material market. Its chemical formula was polycarboxylic acid. Fine river sand was also purchased from the building material market, and it underwent a meticulous screening process prior to its application. The particles with sizes ranging from 24 to 40 mesh and those smaller than 40 mesh were sieved specifically for grout production. Sulfuric acid of analytical purity was procured from Sinopharm Chemical Reagent Co. The water utilized in this study was deionized water.

Design of grout

The composition and proportion of the grout used in this study was listed in Table 2. It had a cement-to-sand ratio of 1:1, a water-to-cement ratio of 0.45, and a water reducer content of 0.5%. This formulation had undergone laboratory testing and field trials, with detailed evaluations conducted on its fluidity, stability, water resistance, strength and other key parameters as reported in prior work [13, 38].

The mixing procedure for the grout was adapted from the procedure described in Baltazar et al. [39]. The operation was as follows: The cement and sand were first premixed, followed by the dissolution of water reducer in a predetermined proportion of water. Subsequently, the solution containing the water reducer is added while stirring, ensuring continuous stirring for 5 min to achieve thorough mixing.

Specimen preparation

Two dimensions of specimens were prepared: a cylindrical specimen measuring 2 cm in diameter and 1 cm in height, and a standard cube specimen with dimensions of 5 cm for length, width, and height. Non-standard cylindrical specimens were utilized specifically for conducting simulated corrosion tests simulating acid rain conditions. The choice of smaller-sized specimens was made to minimize the potential impact of specimen size on ion dissolution during these experiments. On the other hand, standard cube specimens were employed to evaluate compressive strength according to standard ASTM C109 [40]. The specimen production process was as follows: the grout was injected into the iron mold while being stirred, and after 1 d, the mold was removed. Then, the specimens were transferred to a controlled environment with relatively constant temperature and humidity (T = 22 ± 3 °C, RH = 80 ± 5%) for maintenance for a duration of 28 d. Subsequently, corresponding tests and examinations were conducted.

Table 2 The composition and proportion of designed grout

Raw material	Cement	Aggregate (quartz)		Water	Water reducing agent
		24-40mesh	< 40 mesh		
Proportion	1	0.5	0.5	0.3	0.005

Compressive strength test

The cured standard cube specimens were submerged in three sulfuric acid solutions (pH = 3, 4, 5, and 6.5) for several days under 20, 30, 40 and 50 °C temperature regimes. Therefore, a total of 16 series of test specimens would be investigated (four temperature levels and four pH levels). After soaking for 7, 15 and 30 days, the specimens were retrieved for testing and air-dried in lab environment for a period of 2 days. Finally, their compressive strength was measured using an electronic universal testing machine (CMT 5205, SUST, China).

Corrosion procedure

Simulated acid rain

The simulation of sulfuric acid rain was conducted in this study, as it is prevalence in various regions worldwide. The acidic solutions with pH values of 1.3, 2.0, 3.0, 4.0, 5.0, and 6.5 were prepared by dissolving analytical grade sulfuric acid in varying proportions of water. The errors of the pH values were controlled in the range of ± 0.04 by using a digital pH meter (Mettler-Toledo International Trading Co., Shanghai).

Temperature

Revisiting the research on concrete erosion [41], the combined impact of temperature and acid on the grout was tested. The temperatures in the corrosion were 20, 30, 40, and 50 °C. Consequently, when combined with

Table 1 The composition of cement

Sample	Elements (Wt %)						
	Ca	Si	Al	K	Mg	O	S
OPC	29.28	16.32	4.40	1.69	1.23	46.36	0.71

varying concentrations of simulated acid rain, a total of 24 corrosion experimental groups were established.

Procedure

According to the previous work [36], the immersion method was employed in this work to expedite the degradation of cement grouting materials under acidic rainfall. For each corrosion experimental group, 600.00 ± 0.05 g acid solution and 3 specimens were used to mimic 10000 mm rainfall in nature (equivalent to 10 years of natural acid rain erosion) [42]. The cyclic process was as follows (Fig. 1): firstly, the specimens were immersed in an acid solution at a constant temperature. Secondly, after 24 h, the pH value and Ca^{2+} concentration of the acid solution were measured using a pH meter and calcium ion meter respectively. Thirdly, the acid solution was refresh and the specimens were dried at room temperature for 2 h before starting a new cycle. This cycle was repeated for a total of 30 times.

Results and discussion

Compressive strength

In many studies, compressive strength was often used to evaluate the failure of cement [29]. Therefore, the compressive strength of the specimens was also assessed following immersion in a solution at various temperatures and pH levels for a specific duration. The compressive strength of the specimens, after immersion in a solution at 20 °C with a pH value of 6.5 for 7, 15, and 30 days, was measured to be 32.4, 45.7, and 44.1 MPa, respectively. This change in strength could be attributed to water infiltration into the specimen matrix, leading to an increased degree of cement hydration within the test specimen. In order to more clearly reflect the variations in specimen strength under different conditions, the compressive strength value of the aforementioned specimens was adopted as the baseline, and deviations from this baseline under alternative conditions were utilized to assess the impact of temperature, pH value, and soaking time on compressive strength (D-value of compressive strength). The corresponding results were presented in Fig. 2.

The results demonstrated that at a pH of 6.5, the D-value exhibited positive correlation with temperatures of 30, 40, and 50 °C. This phenomenon could be attributed to the direct relationship between temperature and cement hydration rate [28]. When the pH value was below 6.5, conversely, an increase in temperature generally leaded to a decrease in the compressive strength of the cement specimen. This observation indicated that acid corrosion of cement intensified with rising temperatures. Furthermore, in the experimental group maintained at a temperature of 20 °C, we observed a positive increase in the D-value of compressive strength of the specimens after being immersed for a duration of 7 days. This phenomenon was also reported by Okochi et al. and explained as that acid rain might protect mortar and concrete structures from the neutralization during a short period through disturbing the acidic gas-phase diffusion into their interior [43]. It was noteworthy that the law observed in the strength data differ from those observed in the subsequent calcium ion dissolution experiment (Fig. 6). Specifically, we discovered a negative correlation between pH value and the extent of calcium ion dissolution during our experimental investigation. The experimental groups at the other three temperatures did not exhibit a discernible correlation between strength and soaking time.

In summary, the compressive strength of the cement specimen was influenced by factors such as corrosion and neutralization protection provided by solutes

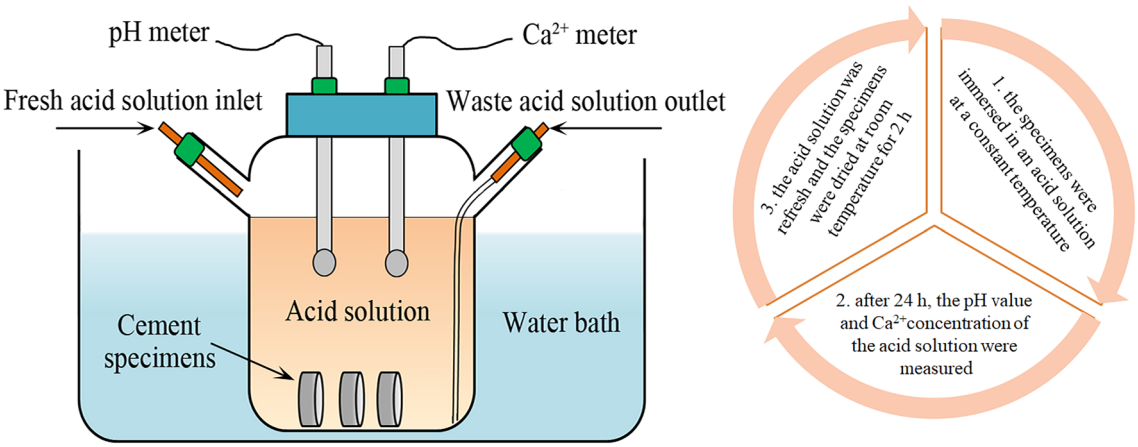

Fig. 1 The cyclic process of accelerated simulated acid rain aging

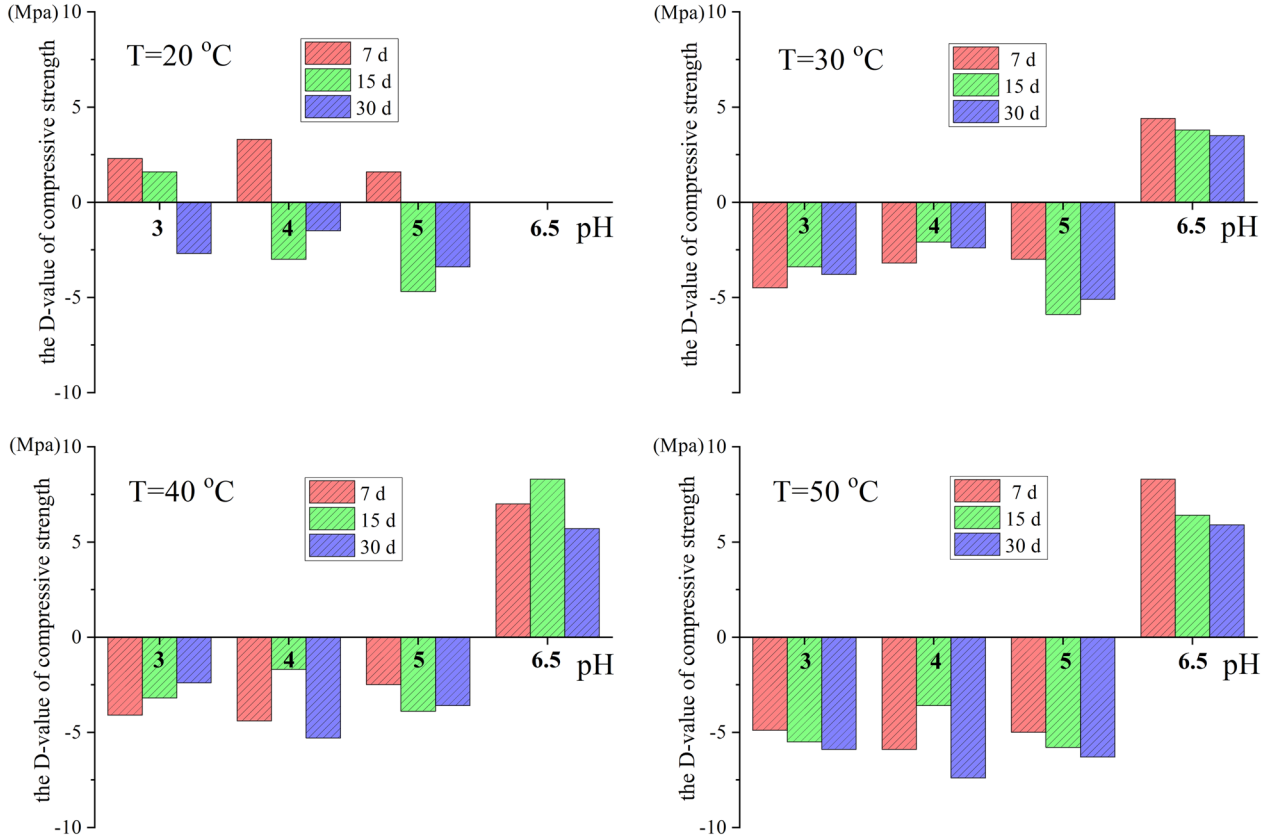

Fig. 2 The D-values of the compressive strengths of the cement samples at different conditions (the compressive strengths of specimen under T = 20 °C and pH = 6.5 as the baseline)

(vitriol) in the soaked solution, as well as both positive effects (hydration promotion) and negative effects (dissolution of soluble ions) caused by water. Therefore, using compressive strength to evaluate the corrosion of cement was insufficient.

Dissolution of Ca^{2+}

In light of the uncertainty surrounding the assessment of cement-based grout's compressive strength against acid erosion, we would employ material loss as a means to evaluate the process henceforth. In this regard, we draw upon previous research [34, 44] and utilize calcium ions as our reference material.

It was important to note that the activity of Ca^{2+} in the solution was omitted, i.e., activity coefficient was 1, for simplifying the calculation. The dissolving-out amount of Ca^{2+} and its relationship with time at different conditions were calculated and shown in Figs. 3, 4, respectively. These calcium ions might be generated from the hydration products of cement, such as calcium hydroxide, tobermorite, and hydrated calcium aluminate, and unhydrated cement clinker, when exposed to acid [34, 45–47]. Thus, we used formula (1) to generalize the calcium ion

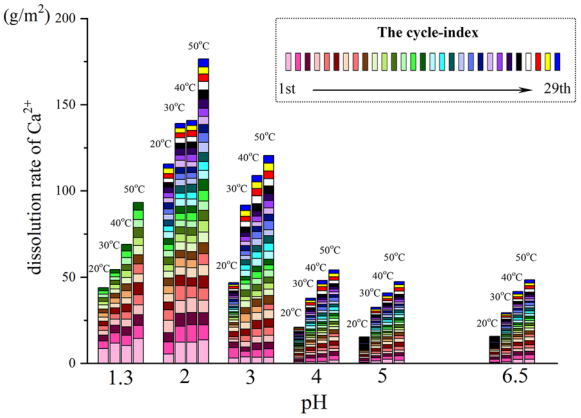

Fig. 3 The dissolving-out amount of Ca^{2+} under different condition

dissolving-out from the cement specimens in aqueous solutions.

$$Ca^{2+}(s) + H^{+}(l) - - - - - - - - Ca^{2+}(l) + H_2O \quad (1)$$

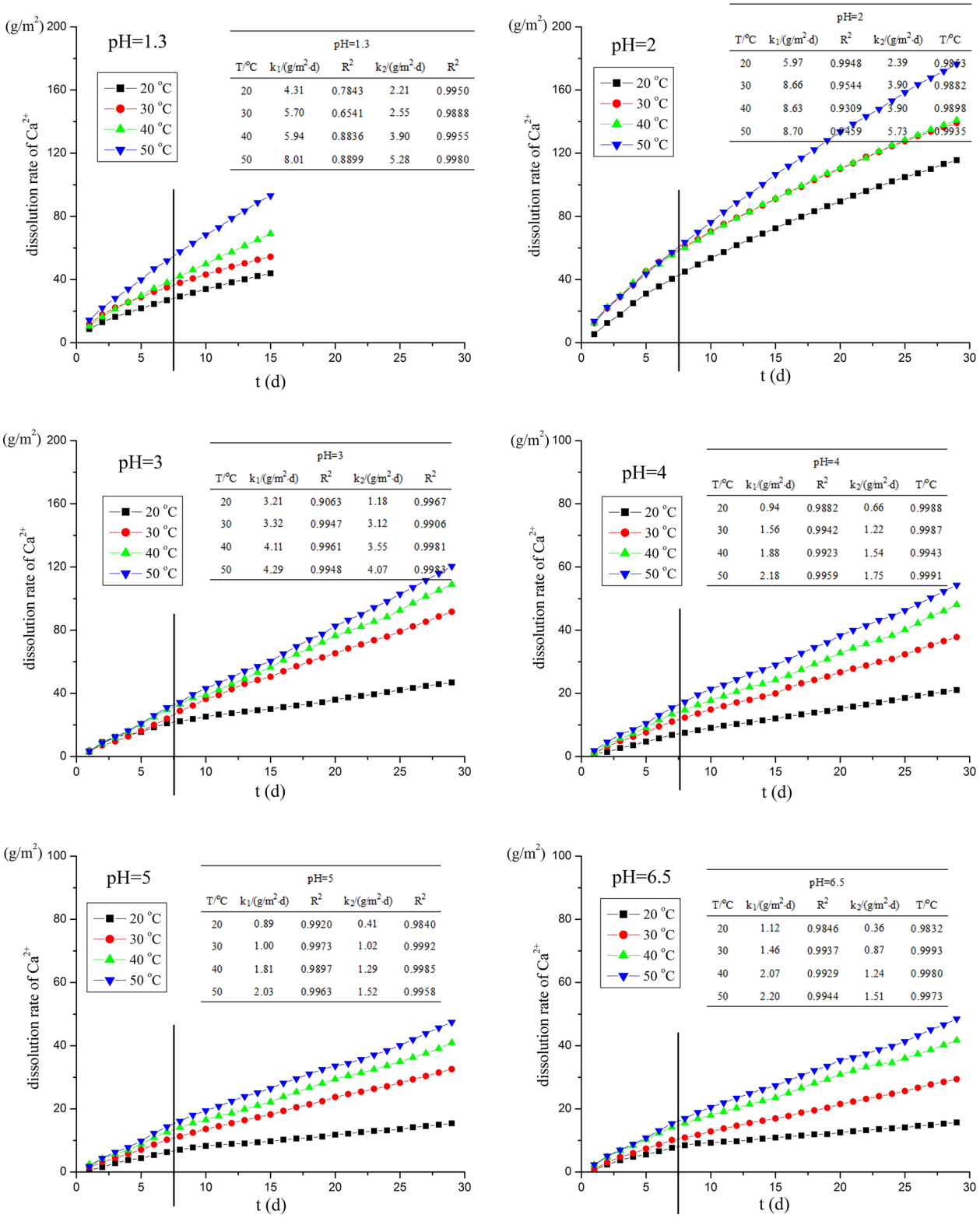

Fig. 4 The dissolution rate of Ca^{2+} with time and the rate constant of reaction at different condition

First, the dissolving-out amount of Ca^{2+} increased as the pH value decreased and temperature increased, as shown in Fig. 3. This phenomenon was particularly evident at lower pH values (≤ 3.0) or lower temperatures (≤ 40 °C). Conversely, when the pH value approached 6.5, there was little change in the dissolution rate of Ca^{2+}. This was due to acidic attack of cement was based on the alkalinity of cement through acidic-alkaline reaction [47]. Additionally, rapid dissolution of Ca^{2+} occurred during the initial cycles. It was worth noting that at a pH of 1.3, only 15 cycles were observed due to both chemical and physical damage (sulfate crystallization) inflicted on the specimen under this condition, causing the specimen to fall apart after 15 cycles, which would be discussed below.

Second, the dissolution rate of Ca^{2+} as a function of time, depicted in Fig. 4, was utilized to analyze the temporal variation in the release of Ca^{2+}. The results demonstrated a linear or approximately linear correlation between the dissolution of Ca^{2+} and time, adhering to formulas (2) and (3). This means the dissolution of Ca^{2+} from cement specimens in acidic solutions followed a zero-order reaction.

$$dc_{Ca}/dt = kc_{Ca,0} \tag{2}$$

$$c_{Ca} - c_{Ca,0} = kt \tag{3}$$

where $c_{Ca,0}$ is the original concentration of Ca^{2+} in the solution, c_{Ca} is the real-time concentration of Ca^{2+} in the solution, k is the rate constant of reaction, and t is the time of reaction.

Based on the zero-order reaction, the k value of formula (1) was calculated and presented in Fig. 4.

The results indicated that the k values prior to the seventh cycle (k_1) were 1.5–2.5 times higher than those after the seventh cycle (k_2), suggesting a greater rate of Ca^{2+} dissolution during the initial seven cycles compared subsequent ones. Furthermore, the dissolution rate of Ca^{2+} exhibited a tendency to reach a stable state after the seventh cycle, as indicated by a linear fitting coefficient exceeding 0.99. During the cement's exposure to acidic conditions, the primary target was calcium hydroxide, which underwent an acid–base neutralization reaction. The resulting soluble calcium salt continued to leach away by the aqueous solution, thereby increasing the porosity within the cement and promoting corrosion progression from the surface towards the interior. Simultaneously, due to this acid–base neutralization reaction, the pH value of cement pore solution decreased, leading to compromised stability of hydration products in the cement matrix. Consequently, gradual decomposition of these calcium-containing and acid-unstable hydration products (like tobermorite, xonotlite, C_3AH_6, C_4AH_{13}, ettringite, gehlenite hydrate and hydrogarnets) occur [47]. Thus, the dissolution of calcium ions was a stepwise manner, elucidating the rapid initial stage of dissolution followed by reaching equilibrium in this experiment. And in several other studies and models [45, 48], a gradual acid erosion of cement had also been observed.

Comparing the values of k_2, the reaction rate constant had no prominent difference at the same temperature when the pH value reached 4.0 (4.0–6.5 in this work). It seems that the dissolving-out rate of Ca^{2+} was mainly controlled by the temperature in this period. When the pH value dropped to 3.0, the value of k_2 increased rapidly. The pH value of ~ 3.0 was considered as the critical point of cement corrosion [33, 49]. Thus, the dissolving-out rate of Ca^{2+} was mostly controlled by the temperature when the pH value of the acid solution exceeded 3.0. Otherwise, it was controlled by both temperature and the pH value of the acid solution.

The relationship among k_{Ca}, T and pH value

To reveal the relationship among k_{Ca} (only k_2 in this part), T and the pH value, the relation between k_{Ca} and T at the same pH value was first calculated. In the preceding section, it was determined that acid attacked on cement occur in two stages based on the reaction rate constant in this study. In this section, the focus of our evaluation lied primarily on k_2, as it offered a more comprehensive reflection of the long-term corrosive impact of cement. The results of the linear fitting were presented in Table 3, demonstrating a strong linear correlation between k and lnT. A simplified formula (4) was obtained when the relationship between k and lnT was further modified and simplified. This formula summed up the relationship among k_{Ca}, T, and the pH value. When the pH was within the limits, the values of A and B were constant (listed in Table 4). This simplified formula could help us estimate the dissolving-out rate of Ca^{2+} when the cement suffers from acid rain with a certain pH value at a temperature.

Table 3 The relation between k and T under the same pH value

pH	Fitting function	Modified function	Simplified function
1.3	k = 3.31lnT-8.09	k = 1/2π·(20.82lnT-50.31)	k = 1/2π·A·(7.5lnT-14-B·pH)
2	k = 3.22lnT-7.31	k = 1/2π·(20.25lnT-45.97)	
3	k = 3.09lnT-7.83	k = 1/2π·(19.43lnT-49.24)	
4	k = 1.19lnT-2.89	k = 1/2π·(7.53lnT-18.23)	
5	k = 1.20lnT-3.15	k = 1/2π·(7.58lnT-19.88)	
6.5	k = 1.25lnT-3.41	k = 1/2π·(7.87lnT-21.29)	

Table 4 The parameters of formula at different pH values

pH	A	B	pH	A	B
7	1	1	3	2.65	2
5	1	1	2	2.65	2
4	1	1	1	3	2

$$k_{\mathrm{Ca}}/\left(\mathrm{g/m^2}\right) = 1/2\mathrm{p} \times \mathrm{A} \times [7.75 ln \mathrm{T}/^{\mathrm{o}}\mathrm{C} - (14 + \mathrm{B} \times \mathrm{pH})] \quad (4)$$

In order to validate the accuracy and applicability of the simplified formula (4), we utilized MATLAB software to generate a 3D map based on the simplified formula (4) and incorporated our experimental measurements into it. The outcomes were illustrated in Fig. 5. The 3D map showed that the curved surface was relatively flat when the pH value changed from 4.0 to 6.5. And the experimental values of *k* were mostly on the curved surface in this range. This implied that within this range, the simplified formula (4) exhibited a high degree of accuracy in predicting the dissolution rate of calcium ions in cement under acid rain erosion. When the pH value decreased to 3.0, the curvature of the surface became significantly steeper. As the pH value decreased further, there was a greater deviation observed between the experimental values of *k* and the curved surface. The findings indicated that the simplified formula (4) was no longer applicable under low pH level. In general, within the pH range of 2 ~ 7, the simplified formula (4) provided a more accurate estimation for calculating the calcium dissolution rate of cement materials under acidic rain conditions. Furthermore, due to insufficient data available between pH 3 and 4, there was a lack of clarity regarding any changes or turning points between these two surfaces, necessitating further.

The pH value of acid solution

Acid solution (H^+) could react with calcium hydroxide (C-H), tobermorite (C-S-H), hydrated calcium aluminate (C-A-H) and other components in cement, via formulae (4), (5), and (6), respectively. If we assumed that 1 mol H^+ reacted with cement could lead to 0.5 mol dissolving-out Ca^{2+}, the consumed H^+ was 2 times as the dissolution of Ca^{2+}. The relationship between the consumed amount of H^+ and the dissolving-out amount of Ca^{2+} was shown in Fig. 6. It could be seen that the pH value of 3.0 appeared to serve as the critical threshold. At this point, the consumed amount of H^+ was nearly 2 times as much as the dissolution of Ca^{2+}. When the pH value was below 3.0, the consumed amount of H^+ was much more than the dissolving-out amount of Ca^{2+} and this trend was more prominent for longer time and lower pH values. This might be caused by the reaction between Ca^{2+} and SO_4^{2-} in formulae (7) and (8), which formed calcium sulfate ($CaSO_4$) precipitate, as sulfuric acid rain was simulated in this work. According to thermodynamics, when the concentration of SO_4^{2-} reached 6.7 mmol/L and the pH value was 1.87 in this work, the $CaSO_4$ precipitate appeared [26, 34]. In Fig. 5, the measured *k* values were consistently smaller than those predicted by the simplified formula (4), indicating a potential influence of calcium ions precipitating with sulfate. On the contrary, when the pH value was larger than 3.0, the reverse was true. In this range, the consumed amount of H^+ was nearly 2 times as much as the dissolving-out amount of Ca^{2+} in the first several days. Afterwards, the consumed amount of H^+ became smooth while the dissolving-out amount of Ca^{2+} increased linearly and exceeded the

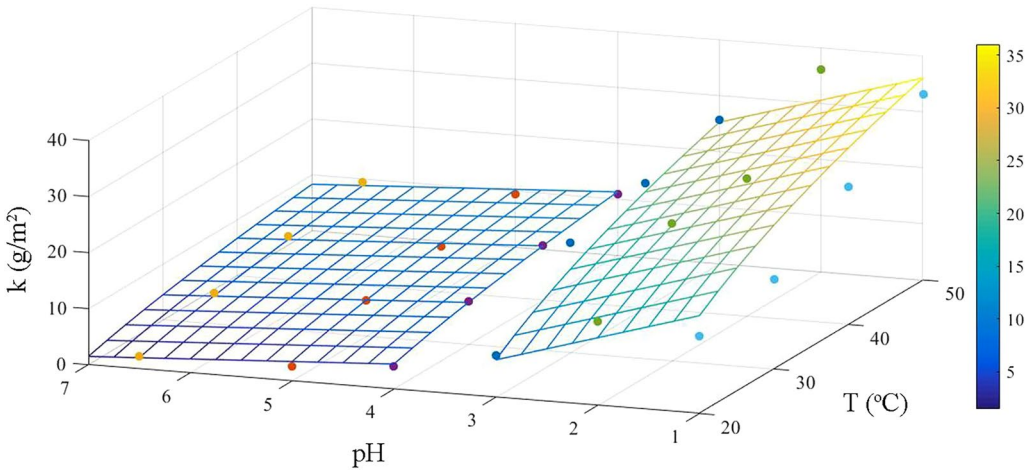

Fig. 5. 3D map of the relationship among *k*, the pH value, and T using formula (4) with experimental data

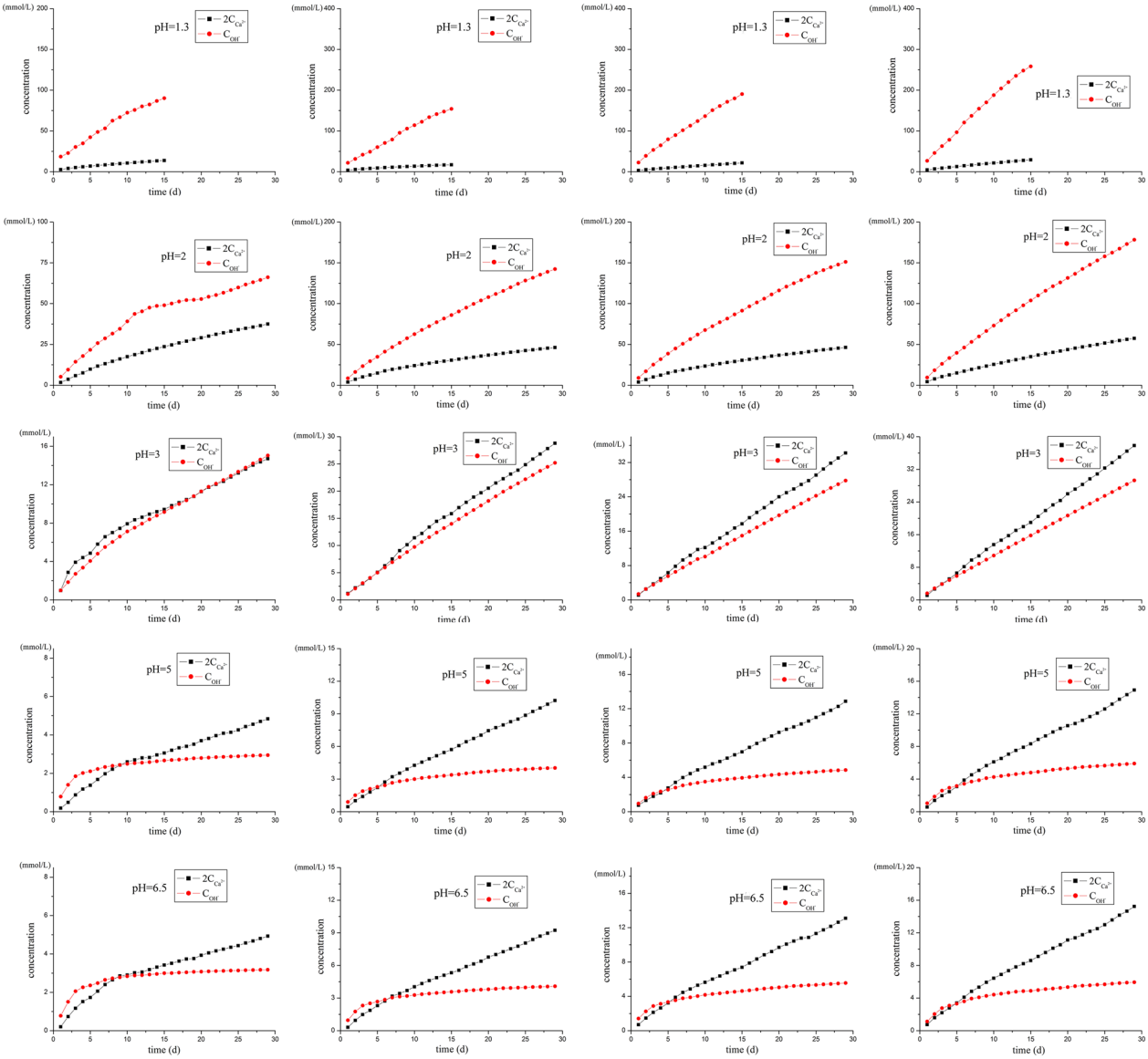

Fig. 6 The relationship between the consumed amount of H^+ and the dissolving-out amount of Ca^{2+}

consumed amount of H^+. This might be because the acid solution was not strong enough to erode C-S-H, C-A-H and other components in cement. It could only react with C-H on the surface of the cement specimens, which was slow to proceed.

$$C-H + H^+ \text{- - - - -} Ca^{2+} + H_2O \quad (4)$$

$$C-S-H + H^+ \text{- - - - - -} Ca^{2+} + SiO_2 + H_2O \quad (5)$$

$$C-A-H + H^+ \text{- - - - - -} Ca^{2+} + Al_2O_3 + H_2O \quad (6)$$

$$Ca^{2+} + SO_4^{2-} + H_2O \text{ - - - - - -} CaSO_4 \times 2H_2O \quad (7)$$

$$CaSO_4 \times 2H_2O + C-A-H + H_2O \text{ - - - - - -} AFt \quad (8)$$

where C-H is calcium hydroxide, C-S-H is tobermorite, C-A-H is hydrated calcium aluminate, and AFt is ettringite.

Conclusion

In this work, we adopted the dynamic method of calcium dissolution rate measurement to study the service life of cement-based grout materials. Through the

simulated acid rain erosion experiment, we found that the dissolution process of Ca^{2+} ions conformed to the 0 order reaction, and the reaction rate was related to the acidity and temperature of acid rain. When the acid rain pH > 3, we could use the formula "$k_{Ca}/(g/m^2) = 1/2\pi \cdot A \cdot [7.75 ln T/^{o}C - (14 + B \cdot pH)]$" to predict dissolution rate of calcium ions. Considering that the acid rain with pH < 4 was relatively few in cultural relics protected area, the above formula could be used to evaluate the failure of general cement grouting materials.

Comparing with the previous studies, this work provides a facile and quantitative method to predict the service life of cement-based grout. In significant conservation projects, a comprehensive investigation and evaluation of conservation methods were conducted prior to implementing ontological conservation work. However, achieving detailed experimental research and investigation on less important cultural relics became challenging due to due to financial and time constraints. Therefore, it was pragmatically significant to establish an intuitive and simplified prediction formula [50].

In the grouting protection of masonry, the grouts should be designed based on the characteristics of the protected object and the desired protective outcome. Therefore, in fact, there are many kinds of grouts. This work exclusively evaluated the commonly used cement-based grouts for rock-carved relics protection, while acknowledging the need for further experimentation to validate the empirical formula derived from this research. Simultaneously, as artificial intelligence technologies such as robot learning become increasingly prevalent in cultural relics preservation [51], we also aspired to integrate these experimental data with interdisciplinary research utilizing said technologies. This would enable more accurate predictions of grouting material lifespan and enhance the safety of cultural relics protection.

Abbreviation

EDS Energy dispersive X-ray spectrometer

Acknowledgements

Not applicable.

Author contributions

WH: Investigation, Experiment, Writing- Original draft preparation. SF: Methodology, Data analysis, Writing- Reviewing and Editing. LX and XC: Data analysis, Preparing pictures and tables. BZ: Conceptualization, Writing- Reviewing and Editing.

Funding

This research is supported by Zhejiang Provincial Administration of Cultural Heritage (2022019).

Availability of data and materials

Available upon request by the authors.

Declarations

Ethics approval and consent to participate

This article does not contain any studies with human participants or animals performed by any of the authors.

Consent for publication

The consent for the publication of details and images in the manuscript are obtained from all participants.

Competing interests

No part of this paper has been published or submitted elsewhere. No competing interests exits in the submission of this manuscript. We acknowledge that this paper has complied with the submission declaration, and any necessary permission has been obtained. The authors declare that they have no known competing financial interests or personal relationships that could have appeared to influence the work reported in this paper.

Received: 19 July 2023 Accepted: 8 November 2023
Published online: 16 November 2023

References

1. Bagde MN. Characterization of failure modes and planned stabilization measures for the Ajanta caves in India. Int J Rock Mech Min Sci. 2016;81:12–8.
2. Frodella W, Elashvili M, Spizzichino D, Gigli G, Adikashvili L, Vacheishvili N, Kirkitadze G, Nadaraia A, Margottini C, Casagli N. Combining infrared thermography and UAV digital photogrammetry for the protection and conservation of rupestrian cultural heritage sites in Georgia: a methodological application. Remote Sens. 2020;12(5):892.
3. Lee CH, Jo YH, Kim J. Damage evaluation and conservation treatment of the tenth century Korean rock-carved Buddha statues. Environ Earth Sci. 2010;64(1):1–14.
4. Margottini C, Antidze N, Corominas J, Crosta GB, Frattini P, Gigli G, Giordan D, Iwasaky I, Lollino G, Manconi A, Marinos P, Scavia C, Sonnessa A, Spizzichino D, Vacheishvili N. Landslide hazard, monitoring and conservation strategy for the safeguard of Vardzia Byzantine monastery complex, Georgia. Landslides. 2015;12(1):193–204.
5. Özer F, Söylemez M, İnce İ, Günaydin O. Detection of deteriorations in cultural structures created by carving into low-strength rocks by the non-destructive test (NDT) method. Front Archit Res. 2023;12(4):788–802.
6. Sileo M, Gizzi FT, Donvito A, Lasaponara R, Fiore F, Masini N. Multi-scale monitoring of rupestrian heritage: methodological approach and application to a case study. Int J Archit Herit. 2020;16(3):469–84.
7. Su M, Ma X, Xue Y, Cheng K, Wang P, Liu Y, Yang F. Application of the small fixed-loop transient electromagnetic method in detecting grottoes seepage channel. Environ Earth Sci. 2023. https://doi.org/10.1007/s12665-022-10739-5.
8. Frodella W, Elashvili M, Spizzichino D, Gigli G, Nadaraia A, Kirkitadze G, Adikashvili L, Margottini C, Antidze N, Casagli N. Applying close range non-destructive techniques for the detection of conservation problems in rock-carved cultural heritage sites. Remote Sens. 2021. https://doi.org/10.3390/rs13051040.
9. Fang S, Zhang B, Zhang K. The long-term monitoring and evaluation of cement-based grout used to govern the water seepage of karst caves in China. Herit Sci. 2020. https://doi.org/10.1186/s40494-020-00392-1.
10. Kaşmer Ö, Ulusay R, Geniş M. Assessments on the stability of natural slopes prone to toe erosion, and man-made historical semi-underground openings carved in soft tuffs at Zelve Open-Air Museum (Cappadocia, Turkey). Eng Geol. 2013;158:135–58.
11. Lu K, Li Z, Niu R, Li F, Pan J, Li K, Chen L. Using surface nuclear magnetic resonance and spontaneous potential to investigate the source of water seepage in the JinDeng Temple grottoes, China. J Cult Herit. 2020;45:142–51.
12. Boldini D, Guido GL, Margottini C, Spizzichino D. Stability analysis of a large-volume block in the historical rock-cut city of vardzia (Georgia). Rock Mech Rock Eng. 2017;51(1):341–9.

13. Fang S, Zhang K, Zhang B, Wang L. Evaluation of cement-based grout for reinforcing unsafe rocks of stone carvings at Hangzhou Klippe in China. J Mater Civ Eng. 2019;31(2):05018005.
14. Hu W, Fang S, Zhang B. Techniques to overcome the obstruction of attachments and improve the antiseepage effectiveness of grouting in protecting stone carvings. J Perform Constr Facil. 2021. https://doi.org/10.1061/(ASCE)CF.1943-5509.0001654.
15 Wang J. Visualizing water seepage dynamics in grotto relics via atom-based representative model. Herit Sci. 2023. https://doi.org/10.1186/s40494-022-00832-0.
16. Liu B, Zhang W, Qu J, Zhang K, Han Q. Controlling windblown sand problems by an artificial gravel surface: a case study over the gobi surface of the Mogao Grottoes. Geomorphology. 2011;134(3–4):461–9.
17. An WB, Wang L, Chen H. Mechanical properties of weathered feldspar sandstone after experiencing dry-wet cycles. Adv Mater Sci Eng. 2020;2020:1–15.
18. Barzoi SC, Luca AC. Significance of studying the petrography and mineralogy of the geological environment of old rupestrian churches to prevent their deterioration. A case study from the South Carpathians. J Cult Heritage. 2013;14(2):163–8.
19 Siegesmund S, Gross CJ, Dohrmann R, Marler B, Ufer K, Koch T. Moisture expansion of tuff stones and sandstones. Environ Earth Sci. 2023. https://doi.org/10.1007/s12665-023-10809-2.
20. Wedekind W, López-Doncel R, Dohrmann R, Kocher M, Siegesmund S. Weathering of volcanic tuff rocks caused by moisture expansion. Environ Earth Sci. 2012;69(4):1203–24.
21. Dong GQ. Anchoring the cliff and excavating diversion canal—the reinforcement and water seepage treatment project in Maiji Grottos. China Cult Heritage. 2016;2:5.
22. Yang SJ, Pi L, Fang Y, Zhang JJ, Chen JP, Fan ZL. Research on metakaolin and micro fine cement composite grouting material in Longmen Grottoes. Cave Temples Stud. 2013;1:393–404.
23. Deng ZJ. Review the conservation works in Dazu stone carving in the past 40 years. Sichuan Cult Relics. 1994;11:41–8.
24. Liang G, Hui D, Wu X, Wu J, Zhang D. Effects of simulated acid rain on soil respiration and its components in a subtropical mixed conifer and broadleaf forest in southern China. Environ Sci Process Impacts. 2016;18(2):246.
25. Xin L, Bo Z, Zhao W, Ling W, Xie D, Huo W, Wu Y, Zhang J. Comparative effects of sulfuric and nitric acid rain on litter decomposition and soil microbial community in subtropical plantation of Yangtze River Delta region. Sci Total Environ. 2017;601–602(1):669.
26. Han TC, Wang HQ. Application of thermodynamics to the study of concrete corrosion. J Jiaozuo Inst Technol. 1997;4(16):56–70.
27. Cheng ZF. Study on corrosion test and evaluation of building foundation. Jilin: Jilin University; 2006.
28. Xie S, Li Q, Ding Z. Investigation of the effects of acid rain on the deterioration of cement concrete using accelerated tests established in laboratory. Atmos Environ. 2004;38(27):4457–66.
29. Chen MC, Kai W, Li X. Deterioration mechanism of cementitious materials under acid rain attack. Eng Fail Anal. 2013;27(1):272–85.
30. Zhang LQ, Pan YN, Xu KC, Bi LP, Chen MC, Han BG. Corrosion behavior of concrete fabricated with lithium slag as corrosion inhibitor under simulated acid rain corrosion action. J Clean Prod. 2022;377:21.
31. Huo RK, Li SG, Ding Y. Experimental study on physicochemical and mechanical properties of mortar subjected to acid corrosion. Adv Mater Sci Eng. 2018;2018:11.
32. Kanazu T, Matsumura T, Nishiuchi T, Yamamoto T. Effect of simulated acid rain on deterioration of concrete. Water Air Soil Pollut. 2001;130(1–4):1481–6.
33. Beddoe RE. Modelling acid attack on concrete: Part II. A computer model. Cement Concr Res. 2016;88:20–35.
34. Yuan H, Dangla P, Chatellier P, Chaussadent T. Degradation modeling of concrete submitted to biogenic acid attack. Cem Concr Res. 2015;70:29–38.
35. Rodriguez-Navarro Carlos, Cazalla Olga, Elert Kerstin, Sebastian Eduardo. Liesegang pattern development in carbonating traditional lime mortars. Proc Royal Soc A Math Phys Eng Sci. 2002;458(2025):2261–73.
36. Fan YF, Luan HY. Pore structure in concrete exposed to acid deposit. Constr Build Mater. 2013;49:407–16.
37. Ortega JM, Garcia-Vera VE, Solak AM, Tenza-Abril AJ. Pore structure degradation of different cement mortars exposed to sulphuric acid. Appl Sci. 2019;9(24):13.
38. Fang SQ, Zhang BJ, Wei SL. Evaluatation of the application of cement grout for the reinforcementof ancient, inscribed rocks. Sci Conserv Archaeol. 2017;3:52–9.
39. Baltazar LG, Henriques FMA, Jorne F, Cidade MT. Combined effect of superplasticizer, silica fume and temperature in the performance of natural hydraulic lime grouts. Constr Build Mater. 2014;50:584–97.
40. ASTM, Standard test method for compressive strength of hydraulic cement mortars (using 2-in. or [50-mm] cube specimens). ASTM C109, West Conshohocken, PA: ASTM, 2016.
41. Mahmoodian M, Alani AM. Effect of temperature and acidity of sulfuric acid on concrete properties. J Mater Civ Eng. 2017;29(10):04017154.
42. Gu J, Shi N, Xue G. Climatic variation of rainfall and wet days in Zhejiang. J Appl Meteorol Sci. 2002;13(3):322–9.
43. Okochi H, Hasegawa S, Saito N, Kubota K, Igawa M, Kameda H. Deterioration of concrete structures by acid deposition—an assessment of the role of rainwater on deterioration by laboratory and field exposure experiments using mortar specimens. Atmos Environ. 2000;18:34.
44. Kuhl D, Bangert F, Meschke G. Coupled chemo-mechanical deterioration of cementitious materials. Part I: modeling. Int J Solids Struct. 2004;41(1):15–40.
45. Dyer T. Influence of cement type on resistance to attack from two carboxylic acids. Cement Concr Compos. 2017;83:20–35.
46. Hasan MS, Setunge S, Law DW, Molyneaux TCK. Predicting life expectancy of concrete septic tanks exposed to sulfuric acid attack. Mag Concr Res. 2013;65(13):793–801.
47. Zivica VR, Bajza A. Acidic attack of cement based materials—a review. Part 1. Principle of acidic attack. Constr Build Mater. 2001;15(8):331–40.
48. Yin SH, Yang YF, Zhang TS, Guo GF, Yu F. Effect of carbonic acid water on the degradation of portland cement paste: corrosion process and kinetics. Constr Build Mater. 2015;91:39–46.
49. Ekolu S, Diop S, Azene F, Mkhize N. Disintegration of concrete construction induced by acid mine drainage attack. J S Afr Inst Civ Eng. 2016;58(1):34–42.
50. Vintzileou E. Three-leaf masonry in compression, before and after grouting: a review of literature. Int J Archit Heritage. 2011;5(4–5):513–38.
51. Mishra M. Machine learning techniques for structural health monitoring of heritage buildings: a state-of-the-art review and case studies. J Cult Herit. 2021;47:227–45.

Publisher's Note